Article

Aurora B/AIR-2 regulates sister centromere resolution and CENP-A/HCP-3 organization to prevent merotelic attachments

Yue Wang[1,*], Charmaine Yan Yu Wong[1], and Karen Wing Yee Yuen [1,2,*]

[1] School of Biological Sciences, The University of Hong Kong, Kadoorie Biological Sciences Building, Pokfulam Road, Hong Kong Special Administrative Region, China
[2] School of Biological Sciences, University of Southampton, Building 85, Highfield Campus, Southampton SO17 1BJ, UK
* Correspondence to: Yue Wang, E-mail: eywang@connect.hku.hk; Karen Wing Yee YUEN, E-mail: kwyyuen@hku.hk

Edited by Xuebiao Yao

During cell division, the accurate capture of sister kinetochores that are built on the centromeres of chromosomes by microtubules emanating from opposite spindle poles governs faithful chromosome segregation. To ensure sister chromatids separate correctly, sister centromeres undergo resolution to achieve bipolar orientation prior to microtubule attachments. Failure of centromere resolution increases the frequency of merotelic attachments, with microtubules from opposite poles attaching to the same sister kinetochore, causing lagging chromosome, aneuploidy, and even cancer progression. The Aurora B-mediated tension-sensing machinery to correct erroneous kinetochore–microtubule attachments has been well studied. However, preventative mechanisms to avoid merotelic attachments that occur in the earlier mitotic stage are poorly understood. In this study, we found that inactivation of mitotic kinase Aurora B/AIR-2 increases merotelic attachments in *Caenorhabditis elegans*. On one hand, Aurora B/AIR-2-deficient cells exhibit a delay in the occurrence of centromere resolution and a disruption in targeting condensin II components to chromatin. On the other hand, loss of Aurora B/AIR-2 results in an increased localization of centromeric proteins CENP-A/HCP-3 and M18BP1/KNL-2 as well as the kinetochore protein MIS-12 on chromatin, which may generate ectopic kinetochores causing erroneous attachments. To conclude, this study elucidated that Aurora B/AIR-2 regulates sister centromere resolution and CENP-A/ HCP-3 deposition to actively prevent merotely and chromosome instability in cells.

Introduction

During cell division, the correct capture of poleward-faced sister kinetochores by opposite spindle microtubules facilitates faithful chromosome segregation. The centromere serves as a platform for kinetochore assembly and its position is epigenetically marked by centromeric protein A (CENP-A/HCP-3), a conserved histone H3 variant specifically at functional centromeres in many organisms (De Rop et al., 2012). CENP-A/HCP-3 in

Caenorhabditis elegans undergoes nearly complete turnover on the chromatin across one cell cycle (Gassmann et al., 2012). However, accurately determining the precise timing of CENP-A/ HCP-3 replenishment on chromosomes in *C. elegans* has been challenging. To ensure sister kinetochores are amphitelically attached, meaning that the sister kinetochores are attached to microtubules emanating from opposite spindle poles, it is expected that the duplicated, sister centromeres resolve from one another and localize to opposite surfaces of well-compacted chromosomes before microtubule attachment. The process of sister centromere resolution occurs in G2 phase in mammalian cells with monocentric chromosomes (Brenner et al., 1981; He and Brinkley, 1996), whereas it occurs later in prophase in *C. elegans* with holocentric chromosomes (Buchwitz et al., 1999; Moore and Roth, 2001; Moore et al., 2005). Failure of this process is believed to trigger centromere disorganization, leading

to merotelic attachments and subsequently chromosome mis-segregation (Stear and Roth, 2002; Wang et al., 2022). Defects of this nature can result in aneuploidy and even cancer progression (Cimini, 2008).

Aurora B kinase, along with three regulatory subunits (INCENP, Survivin, and Borealin), forms the chromosome passenger complex (CPC), which has multiple functions in mitosis (Carmena et al., 2012). In mammals, the CPC complex is recruited to chromosomal arms in early prophase. From late prophase to metaphase, it is enriched at the inner centromere, a site between sister centromeres, that functions as the centromere-signaling network for multiple mitotic events, including kinetochore assembly, stability of the bipolar mitotic spindle, and control of the spindle checkpoint (Adams et al., 2001; Carmena et al., 2012; Trivedi and Stukenberg, 2016). In anaphase, the CPC moves to the mitotic spindle midzone and then remains in the midbody of telophase cells, where it regulates spindle dynamics, cleavage furrow formation, and completion of cytokinesis (Baldini et al., 2016). Aurora B/AIR-2 appears to have functional differences in mitosis and meiosis. Aurora B/AIR-2 is essential for centromere bipolar orientation of sister kinetochores by recruiting condensin components in mitosis (Moore et al., 2005). It acts to resolve chiasma and separation of homologous pairs of chromosomes, through spatially regulating the cleavage of cohesin distal to chiasma in meiosis I (Kaitna et al., 2002; Collette et al., 2011).

Erroneous attachments on kinetochores usually occur during prometaphase when microtubules extend from centrioles and begin to capture the centromeres of sister chromatids after nuclear envelope breaks down (NEBD). Merotelic mis-attachments, where microtubules from opposite poles attach to the same sister kinetochore, often result in sister chromatid separation delay, chromosome mis-segregation, and aneuploid daughter cells. Albeit improper attachments are frequently observed in healthy cells, they can be repaired before metaphase through the spindle checkpoint activation and kinetochore–microtubule correction machinery (Tanaka, 2010; Kuhn and Dumont, 2017). One of the major roles of CPC is to correct the erroneous kinetochore–microtubule attachments by disrupting attachments with improper pulling tension, and in turn promoting new lateral attachment, until achieving stable amphitelic attachments on sister centromeres (Kalantzaki et al., 2015; Doodhi et al., 2021). Furthermore, Aurora B/AIR-2 has been demonstrated to function through several key kinase substrates for error correction (Walczak and Heald, 2008; McVey et al., 2021). One is through regulating mitotic centromere-associated kinesin (MCAK) (Andrews et al., 2004; Ohi et al., 2004; Krenn and Musacchio, 2015). Aurora B fine-tunes the activity of MCAK, providing graded levels of microtubule depolymerase activity (McHugh et al., 2019). Another machinery depends on the Aurora B phosphorylation function on the outer kinetochore components, NDC80 and DAM1C, to promote the disruption of erroneous attachments (Cheeseman et al., 2006; Kalantzaki et al., 2015; Jenni and Harrison, 2018; Doodhi and Tanaka, 2022).

The collaboration between condensin I (consisting of structural maintenance of chromosome (SMC) units SMC-2 and SMC-4 as well as non-SMC units CAP-D2, CAP-G, and CAP-H) and condensin II (consisting of SMC units SMC-2 and SMC-4 as well as non-SMC units CAP-D3, CAP-G2, and CAP-H2) is essential for chromosome condensation and segregation (Hirota et al., 2004; Hirano, 2016). In *Xenopus laevis* and HeLa cells, condensin I and condensing II share a similar distribution pattern, as their localizations are irregularly expanded to the well-condensed chromosome arms (Takao Ono et al., 2004). Additionally, a portion of condensin II is enriched at sister centromere regions (Takao Ono et al., 2004). Without Aurora B activity, the enrichment of condensin II on the centromeric region is lost while defective sister centromere structure is observed in metaphase, implying that condensin II may serve as a regulator to stabilize the centromere structure in mitosis (Takao Ono et al., 2004). On the contrary, Aurora B has been shown to mediate chromosomal structure and segregation by targeting condensin I but not condensin II on mitotic chromosomes in various species, including *C. elegans*, *Drosophila*, and HeLa cells (Giet and Glover, 2001; Lipp et al., 2007; Takemoto et al., 2007; Collette et al., 2011). Notably, in *C. elegans*, condensin I is widely distributed throughout the internal region of mitotic chromosomes, while condensin II predominantly localizes to the outer surface of holocentric chromosomes, aligning with the pattern of centromere protein localization (Hagstrom et al., 2002; Stear and Roth, 2002; Csankovszki et al., 2009). The common component of condensin I and condensin II, SMC-2/MIX-1, and condensin-II-specific CAP-D3/HCP-6 have been determined to assist sister centromere resolution. *mix-1(RNAi)* or *hcp-6(RNAi)* exhibited defects in chromosome condensation and sister centromere resolution, leading to twisted chromosomes and unresolved centromeres in *C. elegans* embryonic cells (Stear and Roth, 2002; Moore et al., 2005). These defects give rise to merotel-ically oriented kinetochores, resulting in the aggravated rate of lagging chromosomes in anaphase (Kaitna et al., 2002). Also, Aurora B/AIR-2 was found to recruit the shared SMC condensin subunits (SMC-2/MIX-1 and SMC-4) on holocentric chromatin (Hagstrom et al., 2002; Kaitna et al., 2002). Contrarily, another study showed that SMC-4 and condensin II-specific component CAP-G2/CAPG-2 targeted to chromosomes normally in AIR-2-deficient embryos, and depletion of AIR-2 merely delayed the mitotic condensation timing instead of altering condensation degree (Maddox et al., 2006). Nonetheless, these results provide hints that Aurora B/AIR-2 may contribute to chromosome structure and centromere organization by recruiting particular condensin subunits to chromatin.

Aside from the Aurora B/AIR-2-regulated pathway, the CENP-A/HCP-3 pathway plays as another critical regulator in assisting resolution of sister centromeres (Moore and Roth, 2001; Moore et al., 2005). Of note, CENP-A/HCP-3 and CENP-C/HCP-4 have been determined to recruit CAP-D3/HCP-6 to holocentric chromatin. The depletion of either CENP-A/HCP-3 or CENP-C/HCP-4 fails to deposit the CAP-D3/HCP-6 on mitotic sister

centromeres, indicating that the inner kinetochore proteins enable the recruitment of CAP-D3/HCP-6 (Stear and Roth, 2002; Chan et al., 2004). In particular, the role of CENP-C/HCP-4 in this process is to remove cohesin protein (SCC-3) from sister centromeres (Moore et al., 2005), promoting sister centromeres to separate from one another. In addition, spindle microtubules have a function in promoting sister centromere resolution after NEBD (Moore et al., 2005), in case aberration occurs in the above-mentioned pathways.

Centromere organization is a key step to ensure centromere bipolar orientation and faithful chromosome segregation. The dearth of knowledge on sister centromere resolution, no matter in mammalian or invertebrate animals, prompts us to discern the mystery behind this process. Several features of *C. elegans* make it a powerful tool for centromere studies (*C. elegans* Sequencing Consortium, 1998; Fire et al., 1998; Kim et al., 2018). The magnified centromere architecture on holocentric chromosomes serves as a prominent feature for centromere resolution and dynamics investigation. This study aims to explore the roles of Aurora/AIR-2 in centromere dynamics, particularly focusing on sister centromere resolution and centromere organization. Our results showed that Aurora B/AIR-2 regulates centromere organization in early mitosis through different ways. Live-cell imaging showed that sister centromeres start to resolve upon pronuclei meeting and achieve bipolar orientation before NEBD. On one hand, this process was extended when Aurora B/AIR-2 function was inactivated. Interestingly, we revealed an additional role of Aurora B/AIR-2 in regulating the localization of condensin II components in mitosis, including CAP-D3/HCP-6, a key factor for sister centromere resolution. On the other hand, cells with inactivated Aurora B/AIR-2 displayed a denser localization pattern of CENP-A/HCP-3 on chromatin fibers, with brighter and enlarged CENP-A/HCP-3 domains. Taken together, our results on the new roles of Aurora B/AIR-2 unravel the preventative mechanism of merotelic attachments in *C. elegans*.

Results

Distinct mitotic defects inspected in the absence of Aurora B/AIR-2 activity

In previous studies, Aurora B/AIR-2 has been demonstrated to be involved in various processes during cell division (Adams et al., 2001; Carmena et al., 2012; Trivedi and Stukenberg, 2016). *air-2(RNAi)* embryos have shown defects in mitotic chromosome segregation and cytokinesis, implying the critical role of Aurora B/AIR-2 for mitotic progression (Severson et al., 2000; Kaitna et al., 2002). Indeed, when employing the RNA interference (RNAi) technique to study the functions of Aurora B/AIR-2, *air-2(RNAi)*-mediated meiotic defects (e.g. multinucleated or polyploid chromosome numbers in one-cell embryos) can be passed onto embryos (Schumacher et al., 1998; Kaitna et al., 2002), rendering it challenging to distinguish the separated roles of Aurora B/AIR-2 in mitosis and meiosis. To investigate the functions of Aurora B/AIR-2 in mitotic progression, particularly in prophase and prometaphase, we utilized a fast-acting,

temperature-sensitive mutant of *air-2*, *air-2(or207ts)*, which can inactivate AIR-2 protein function by shifting temperature to 25°C at a designated time (Severson et al., 2000; Kaitna et al., 2002). Brood size and embryonic lethality rate examination were conducted to test the defects of AIR-2 inactivation in response to different temperature shifts (Supplementary Figure S1A and B). The brood size was reduced significantly when worms were shifted at the L4 stage to 25°C, but not changed when shifted to semi-restrictive temperature 20°C or when kept at permissive temperature 15°C, suggesting that AIR-2's function in germline development is severely affected in *air-2(or207ts)* at 25°C (Supplementary Figure S1A; Severson et al., 2000). The *air-2(or207ts)* mutant exhibited 100% embryonic lethality at both 25°C and 20°C (Supplementary Figure S1B), suggesting that embryonic development is more sensitive to AIR-2 function than germline function.

To bypass the defects inherited from meiosis, we set out to identify the condition that only concerns the mitotic chromosome dynamics in the invariant one-cell embryos. In support of this notion, the temperature shift must be conducted after embryos finish the maternal meiosis II anaphase process, which is ∼11 min before pronuclei meeting in the first mitosis (McCarter et al., 1999; Sonneville and Gonczy, 2004; Oegema and Hyman, 2006). Briefly, a 10-min upshift of temperature from 15°C to 25°C was performed in each *air-2(or207ts)* or wild-type embryo before image acquisition of the first cell division (from pronuclei meeting to anaphase), such that only mitotic defects were quantitatively characterized without any meiotic defects (Figure 1A). Previous studies have also qualitatively described the phenotypic defects in *C. elegans* cells inactivated of AIR-2 (Kaitna et al., 2002; Collette et al., 2011). Abnormality in metaphase chromosome plate formation was inspected in all *air-2(or207ts)* embryos, as compared to a well-aligned metaphase plate formed in wild-type embryos (Figure 1B and C). In anaphase, all *air-2(or207ts)* embryos displayed the separation of two sister chromatid masses, as compared to the partitioning of two sister chromatid rods in wild-type embryos (Figure 1B and C). Near 50% of embryos displayed chromatin bridges in the *air-2(or207ts)* mutant (Figure 1C). Furthermore, time-lapse imaging was performed to record the mitotic events from NEBD to anaphase. The duration from NEBD to anaphase was 232 ± 8 sec in AIR-2-inactivated embryos, compared to only 199 ± 12 sec in wild-type embryos, indicating that an extra 30 sec is required for proceeding NEBD to anaphase in the absence of AIR-2 function (Figure 1D).

We further examined the frequency of merotely in early mitosis, defined as one single sister kinetochore attaches to microtubules emanating from both spindle poles (Figure 1E). To precisely visualize the connection between microtubules and centromeres, we analyzed single Z-plane images of immunofluorescence with centromere and α-tubulin staining. *air-2(or207ts)* embryos showed an increased rate of merotelic attachments in prometaphase, amping up to 60% when compared to the frequency of only 11% in wild-type embryos (Figure 1F). AIR-2 has been shown to influence the localization of
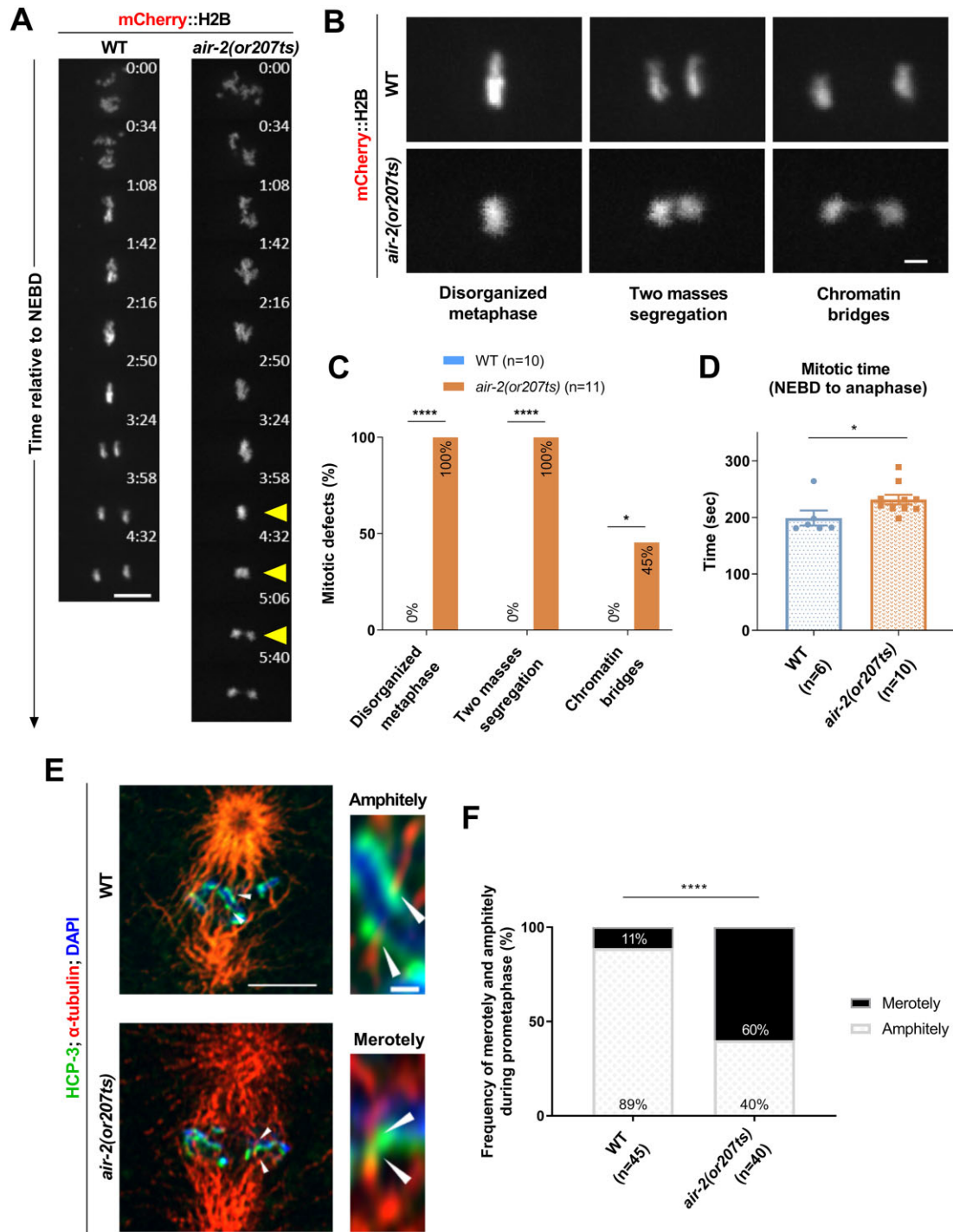
Figure 1 Distinct mitosis defects inspected in AIR-2-inactivated cells. (**A**) Time-lapse micrographs generated from embryos endogenously expressing mCherry::H2B at 25ºC. Scale bar, 10 μm. Relative time to NEBD is shown. Arrowheads indicate three identified mitotic defects. (**B**) Representative images of mitotic defects in *air-2(or207ts)* embryos versus the normal status in wild-type embryos. Scale bar, 3 μm. Mitotic stages and defects were determined as described in detail in Supplementary material. (**C**) Quantification of the respective mitotic defects in embryos. n: number of one-cell embryos examined. *$P < 0.05$, ****$P < 0.0001$, χ^2 analysis. (**D**) Quantification of the average mitotic time (from NEBD to anaphase) during one-cell division. n: number of embryos scored. Error bars: 95% confidence interval (CI) of the standard error of the mean (SEM). *$P < 0.05$, unpaired *t*-test. (**E**) Representative single Z-plane images of amphitelic and merotelic attachments in wild-type and *air-2(or207ts)* embryos. White arrowheads point out the attachment sites. Scale bar, 5 μm (original) or 0.5 μm (magnified). (**F**) Quantification of amphitely and merotely during mitotic prometaphase. n: number of chromosomes analyzed. ****$P < 0.0001$, χ^2 analysis.

condensin, which can impact proper chromosome condensation (Hagstrom et al., 2002; Kaitna et al., 2002). Hence, we were prompted to investigate whether defective condensation occurs when AIR-2 was inactivated. To test this hypothesis, we adopted the condensation measurement approach described previously (Maddox et al., 2006), where the beginning of condensation was indicated by the change of slope in condensation parameter (Supplementary Figure S1C). The final condensation level in *air-2(or207ts)* was comparable to that in wild-type upon NEBD, although the *air-2(or207ts)* mutant showed a higher condensation level at the initial condensation phase (Supplementary Figure S1C), indicating that inactivation of AIR-2 affects condensation dynamics during mitotic progression but not the final level of condensation. In terms of the dynamics, condensation in *air-2(or207ts)* embryos initiated earlier than that in wild-type embryos, as the condensation parameter had progressively increased since 200 sec before NEBD (Supplementary Figure S1C).

Sister centromere resolution is retarded in air-2(or207ts) embryos

To investigate the exact timing of sister centromere resolution, we imaged centromere bipolar orientation by staining centromeres and microtubules in fixed one-cell embryos (Figure 2A). In prophase, a single line pattern of HCP-3 was observed when the two pronuclei proceeded to rotate. Upon NEBD, the bipolar configuration of sister centromeres was fully established before the spindle microtubules were attached. In late prometaphase, microtubules emanated from the opposite poles attached to poleward-facing centromeres. To capture the dynamics, live-cell time-lapse imaging was also performed in two pronuclei to inspect centromere organization during one-cell division (Figure 2B). A single-line architecture of HCP-3 was visualized when the two pronuclei met with one another. From then on, they started to partition, and two rod-like centromeres were discernibly observed when the cell proceeded into the NEBD stage. Taken together, we inferred that sister centromeres start to resolve after pronuclei meeting, and completely achieve bipolar orientation upon NEBD prior to microtubule attachment in *C. elegans* (Figure 2A and B).

As AIR-2 has been demonstrated to be involved in resolving sister centromeres, we further explored whether AIR-2 affects the timing of this event. The mitotic time duration from pronuclei meeting to centromere resolution initiation, the first time frame to observe sister centromeres resolve from one another even only in some parts of the chromosome, was recorded (Figure 2B). The average duration of this mitotic event was measured. It took 34 ± 12 sec and 134 ± 23 sec to drive sister centromere resolution in wild-type and *air-2(or207ts)* cells, respectively. Notably, an extended time ($\sim$100 sec) was required for centromere resolution initiation when AIR-2 function was blocked (Figure 2B), concluding that AIR-2 inactivation leads to retardation of sister centromere resolution. This may contribute to the extension of mitotic time from NEBD to anaphase.

Aurora B/AIR-2 targets condensin II loading on chromatin

In *Drosophila*, *Xenopus*, and HeLa cells, Aurora B has been demonstrated to recruit condensin I to chromosomes (Giet and Glover, 2001; Lipp et al., 2007; Takemoto et al., 2007). In line with these findings, the inactivation of AIR-2 significantly reduced the level of condensin I in *C. elegans* (Supplementary Figure S2A; Collette et al., 2011). This raised our interest in investigating whether AIR-2 also regulates the loading of condensin II in mitosis. We started with monitoring the loading dynamics of CAP-D3/HCP-6 (Figure 3A), which is vital for sister centromere resolution (Stear and Roth, 2002; Moore et al., 2005). CAP-D3/HCP-6 level, as measured by quantification of the GFP::HCP-6 signal from pronuclei meeting to anaphase, dropped by 30% in the *air-2(or207ts)* embryos when compared to that in the wild-type embryos (Figure 3B), suggesting that the loading of HCP-6 to chromatids is partially regulated by AIR-2. Furthermore, signals of the remaining condensin II-specific components, CAP-H2/KLE-2 and CAP-G2/CAPG-2, were traced in the absence of AIR-2 function (Figure 3A and B). Condensin II signals, measured by quantification of the GFP::KLE-2 and GFP::CAPG-2 signals during the first cell division, also dropped significantly when AIR-2 function was blocked, but the timing of this decline seemed to vary (Figure 3A and B). In particular, we found that the CAP-H2/KLE-2 level remained similar to the level in wild-type embryos during pronuclei meeting, but started to drop after NEBD. On the other hand, CAP-G2/CAPG-2 levels remained stable from pronuclei meeting to metaphase, but decreased only at anaphase. These findings indicate that AIR-2 plays an important role in condensin II localization in mitosis.

Yet, whether HCP-6 in turn influences its upstream factor remains obscure. To test this hypothesis, AIR-2 localization in prometaphase was investigated in HCP-6-deficient cells. The chromosomal localization of AIR-2 increased after HCP-6 inactivation (Supplementary Figure S2B), demonstrating that the two proteins indeed affect each other's localization, but the direction of effects is not straightforward to understood and it is unclear whether AIR-2 signal intensity represents its activity.

Aurora B/AIR-2 and CENP-A/HCP-3 coordinately assist CAP-D3/HCP-6 localization for correct resolution

To quantitatively analyze the frequency of distinct centromere types observed during one-cell division in *air-2(or207ts)* and wild-type embryos (Figure 4A), the linescan method was adopted to categorize various centromere organization. A 10-pixel line was drawn to profile the lateral axis of centromere to measure the distribution for GFP-tagged HCP-3, from mono-oriented to bipolar-oriented configurations (Figure 4B and C). Normally, centromeres are displayed as the mono-oriented type in prophase, as reflected by a single peak drawn in the HCP-3 distribution curve (Figure 4C). Then the sister centromeres are resolved and oriented to the poleward faces of chromosomes prior to NEBD, where two symmetric peaks were observed in the HCP-3 distribution curve (Figure 4C). Coincident with the previous studies (Stear and Roth, 2002;
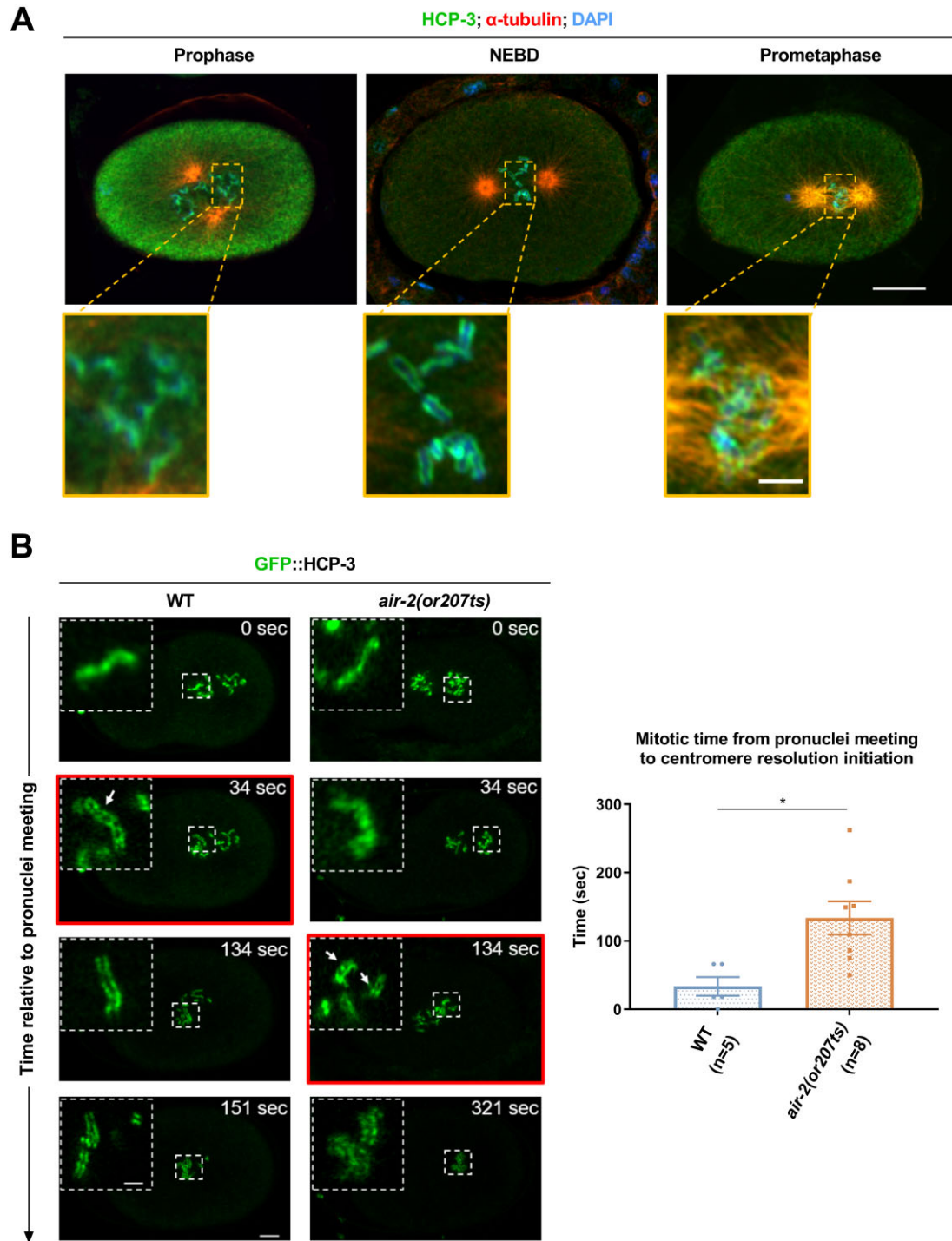
Figure 2 Delayed sister centromere resolution in *air-2(or207ts)* embryos. (**A**) Immunofluorescence staining of HCP-3 and α-tubulin at different cell-cycle stages in one-cell wild-type embryos. The centromere region at each mitotic stage is magnified. Scale bar, 10 μm (original) or 2 μm (magnified). (**B**) Time-lapse images of centromere resolution timing in wild-type and *air-2(or207ts)* embryos. Insets display the enlarged centromere region in a single Z-plane format. The red-frame images show centromere resolution initiation, while arrows in insets indicate the centromeres starting to resolve. Scale bar, 5 μm (original) or 2 μm (inset). The average onset time of centromere resolution initiation was quantified. n: number of one-cell embryos scored. Error bars: 95% CI of the SEM. *$P < 0.05$, unpaired *t*-test.
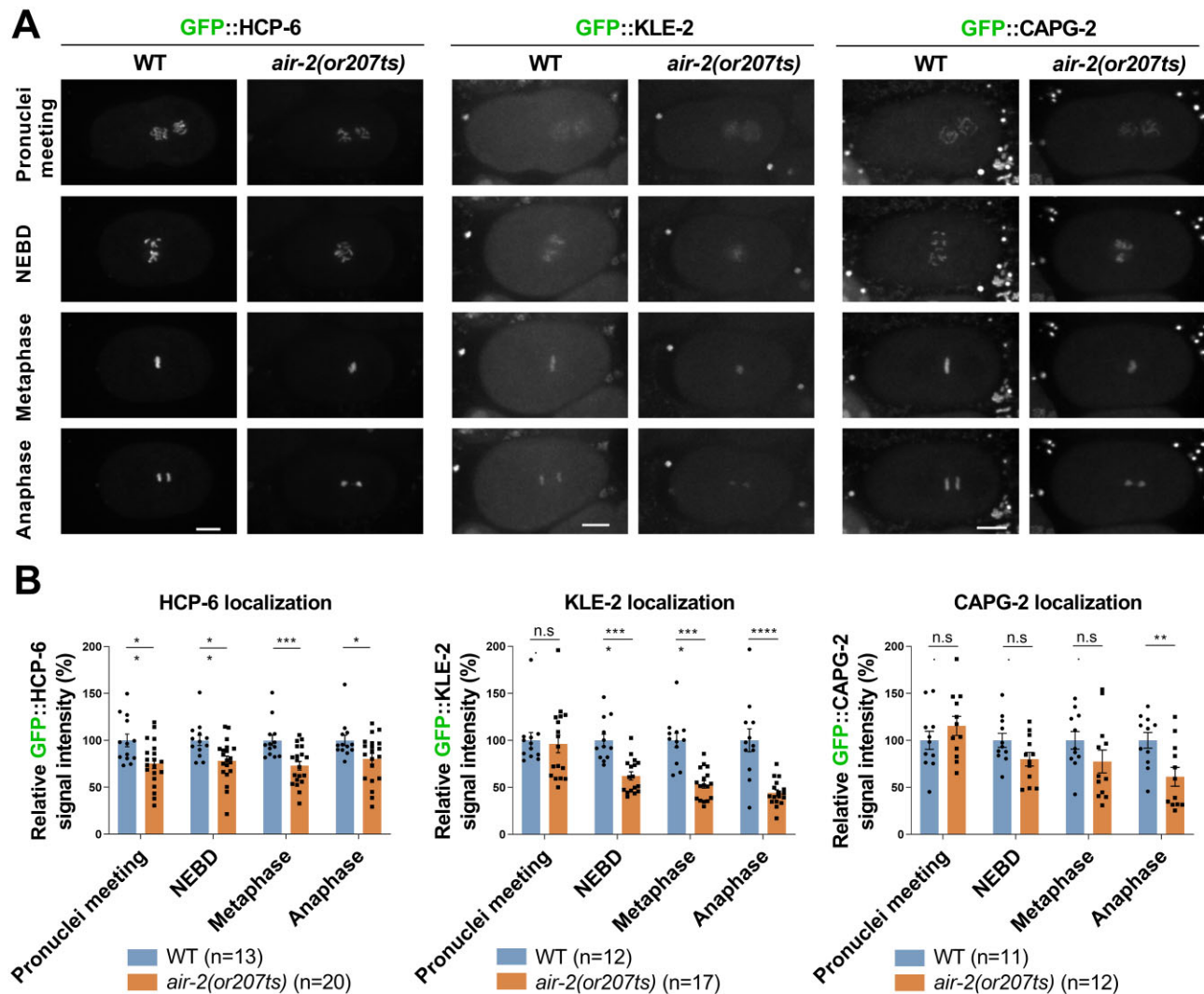
Figure 3 AIR-2 regulates condensin II localization in mitosis. (**A**) Time-lapse images of condensin II non-SMC subunit localization at different mitotic stages in wild-type and *air-2(or207ts)* embryos. Scale bar, 10 µm. (**B**) Comparison of relative condensin II non-SMC subunit signal intensity in wild-type and *air-2(or207ts)* embryos. n: number of one-cell embryos examined. Error bars: 95% CI of the SEM. n.s., not significant; $*P < 0.05$, $**P < 0.01$, $***P < 0.001$, $****P < 0.0001$, unpaired *t*-test.

Moore et al., 2005), disorganized centromeres were seen by the distorted configuration of sister centromeres on chromatin in AIR-2-deficient embryos, as reflected by a broader, unresolved pattern of HCP-3 distribution (Figure 4C). Therefore, three distinct types of centromeres were classified when comparing the lateral HCP-3 distribution within the same width (Figure 4B and C).

Next, we compared the frequency of disorganized centromeres in prometaphase (Figure 4D). At this stage, all of the wild-type embryos achieved bipolar-oriented centromeres, but nearly half (22 out of 48) of the centromeres displayed the disorganized configuration in *air-2(or207ts)* embryos. Approximately 87% (61 out of 70) of disorganized centromere was observed in *hcp-6(RNAi)* cells, which was even higher than the frequency in the *air-2* mutant, suggesting that HCP-6 is not only regulated

by AIR-2. Similarly, 87% (39 out of 45) of centromeres exhibited the disorganized configuration in *air-2(or207ts)hcp-6(RNAi)* embryos, suggesting epistatic interactions between *hcp-6* and *air-2*. In accord with a previous study (Moore et al., 2005), we found that disorganized centromeres occurred in up to 95% (38 out of 40) in *air-2(or207ts)hcp-6(RNAi)* embryos treated with nocodazole, proving that microtubules can rescue the process when the resolution goes awry in the early stage. Thereby, our findings provide more convincing evidence that HCP-6 serves as the key regulator in assisting sister centromere resolution, as recruited by the previously identified HCP-3 pathway (Stear and Roth, 2002; Moore et al., 2005) and the AIR-2 pathway as identified in this study. We cannot perform the triple knockdown of *air-2(or207ts)hcp-3(RNAi)hcp-6(RNAi)* to verify, as the assay requires the monitoring of HCP-3 itself on centromeres.
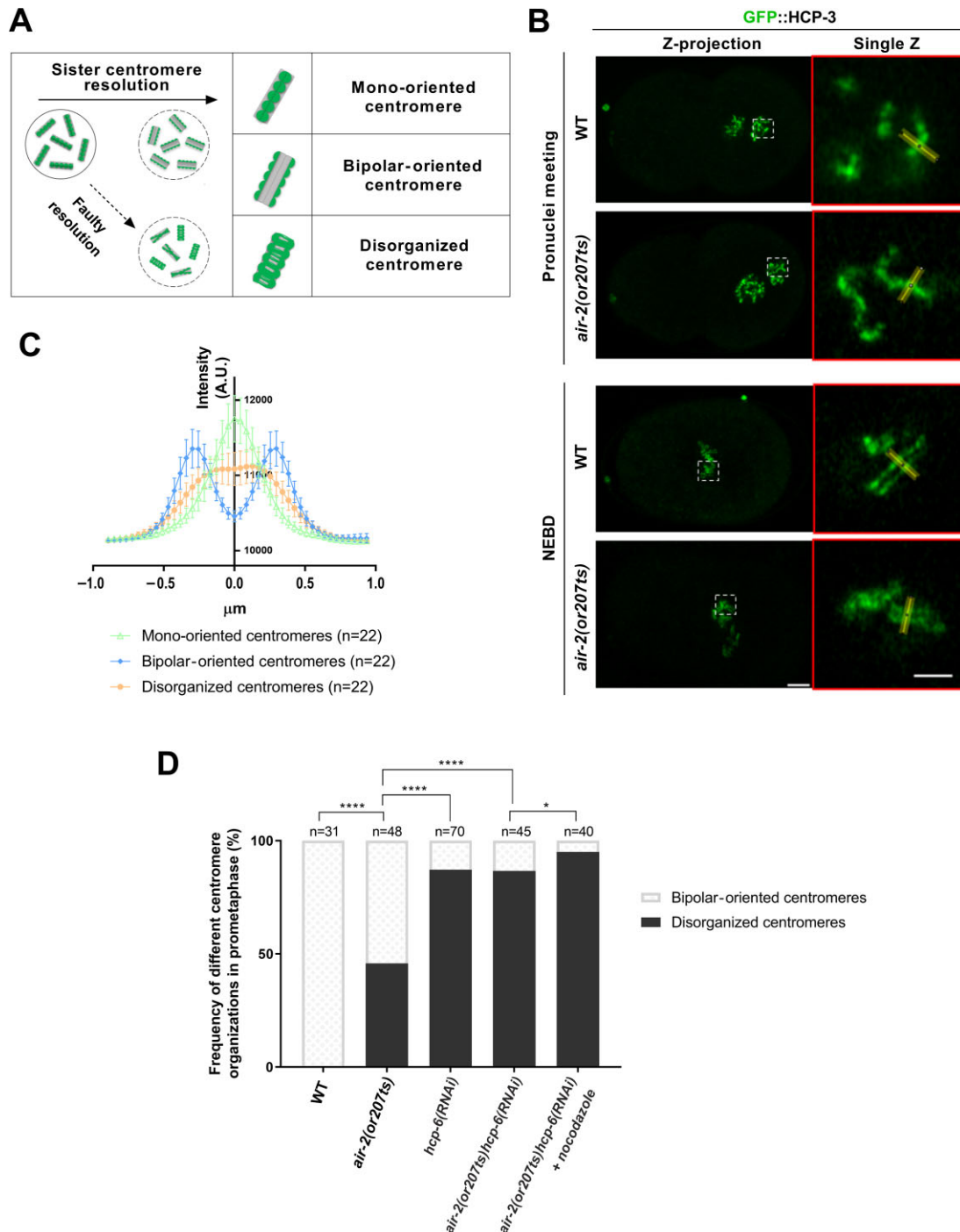
Figure 4 Quantitative measurement of resolved centromere incidences when AIR-2, HCP-6, and MTs are disrupted. (**A**) The schematic illustrates the three types of centromeres during the process of sister centromere resolution. (**B**) Live-cell images of different types of centromeres in wild-type and *air-2(or207ts)* embryos. The red-frame insets show the magnified region highlighted by white dotted lines. Scale bar, 5 μm (original) or 2 μm (inset). (**C**) Linescan profile of GFP::HCP-3 to assess the centromere category. The HCP-3 distribution of each centromere type is plotted. Error bars: 95% CI. n: the number of mono-oriented centromeres in wild-type cells during pronuclei meeting, bipolar-oriented centromeres in wild-type cells during NEBD, and disorganized centromeres in *air-2(or207ts)* during NEBD, respectively. (**D**) Quantification of bipolar-oriented and disorganized centromere incidences in *hcp-6(RNAi)*, *air-2(or207ts)*, and *air-2(or207ts)hcp-6(RNAi)* embryos. Prometaphase refers to the period after NEBD and before metaphase. n: number of centromeres analyzed. $*P < 0.05$, $****P < 0.0001$, Fisher's exact test.

Loss of Aurora B/AIR-2 escalates the localization of CENP-A/HCP-3 on chromatin

In mammals, it was shown that Aurora B possesses a kinase activity on CENP-A at Ser7 residue (Zeitlin et al., 2001). The phosphosite-deficient CENP-A caused defects in kinetochore function and cytokinesis completion, but influenced the cell-cycle progression to a lesser extent (Zeitlin et al., 2001; Kunitoku et al., 2003). In *C. elegans*, we wonder whether AIR-2 also regulates holocentromere organization in addition to sister centromere resolution. High temporal resolution live-cell microscopy was used to track GFP::HCP-3 signal dynamics in the first cell division. After maximally projecting the Z-stack images, brighter GFP::HCP-3 signals on chromosomes were observed during pronuclei meeting, NEBD, and anaphase in AIR-2-inactivated cells (Figure 5A). The average HCP-3 intensity in prometaphase was >1.5 times higher in *air-2(or207ts)* embryos compared to wild-type embryos (Figure 5A), while the average H2B intensity showed no difference between *air-2(or207ts)* embryos and wild-type embryos (Supplementary Figure S3A). This suggests that the loading level of HCP-3 on chromatin is specifically affected, while the levels of other histones remain unchanged. However, total HCP-3 levels in embryonic lysates were comparable in the wild-type and *air-2(or207ts)* cells, as determined by western blotting (Figure 5B), indicating that the steady-state level of the HCP-3 protein is not affected. In addition, HCP-6 depletion resulted in an elevated level of HCP-3 in pronuclei meeting and metaphase (Supplementary Figure S2C). This resembles the impact of AIR-2 on HCP-3 chromatin levels (Figure 5A), suggesting that AIR-2 potentially exerts its influence on HCP-3 through HCP-6.

Having established that the localization of HCP-3 was affected by AIR-2, we continued to test whether KNL-2, the known licensing factor for HCP-3 localization, was also influenced. Immunostaining of endogenous KNL-2 showed that the KNL-2 level in *air-2(or207ts)* was >1.5 times higher than that in wild-type (Figure 5C). As for the outer kinetochore protein MIS-12, immunostaining analysis showed that MIS-12 level in *air-2(or207ts)* nearly doubled (Figure 5C). Together with the presence of merotelic attachments and defective chromosome segregation in *air-2(or207ts)* cells (Figure 1), increased levels of centromere and kinetochore proteins detected in AIR-2-deficient cells suggested that centromeres could be malfunctioning with ectopic kinetochores assembling on the chromatin.

Aurora B/AIR-2 inactivation triggered centromere mis-localization on chromatin fibers

As AIR-2 stays closely between the sister centromeres in mitosis, we postulated AIR-2 might participate in centromere assembly and organization through regulating the centromere protein localization on chromatin. To test this hypothesis, we compared the HCP-3 distribution on chromatin fibers stretched from embryos. The schematic was drawn to depict the method for stretched fiber acquirement and measurement (Figure 6A). Theoretically, H4 is a histone marker to be inspected in every nucleosome, while HCP-3 is assumed to be found only

on some of the centromeric chromatin (Gassmann et al., 2012). DNA staining can directly reflect the status of extended chromatin fiber. Since *C. elegans* possesses a holocentromere distributed along the genome, centromere signals were commonly inspected on multiple sites of most fibers (Figure 6B). Obviously, *air-2(or207ts)* fibers showed a different localization pattern, in which HCP-3 foci appeared to be larger, brighter, and even denser (Figure 6B).

Diverse thicknesses and lengths of stretched fibers were found in sample pools, attributed to the different stretching forces applied. Thus, a post-selection was required to screen out those fibers with a similar stretched status for comparison. A segmented line (25 pixel wide, 30 µm long) was drawn along the fiber (Figure 6A), and the mean intensity of 25-pixel width was calculated along with the points on the line. The width-averaged HCP-3 and H4 pixel intensities along the whole length of the chromatin fiber were sampled and plotted for the two intensities. H4 intensity at 180000–185000 A.U. represented sampled pixels that are on fibers with similar thickness, which were selected for further analysis (Figure 6C). When comparing the R^2 value, the wild-type fibers possessed a value of 0.645, while the *air-2(or207ts)* fibers had a lower value of 0.007, implying that the accretion in HCP-3 signals was less dependent on the H4 level (Figure 6C). To further investigate the HCP-3 domain occupancy on the fiber, only the regions with HCP-3 intensity >181000 A.U. were selected and subsequently determined as HCP-3 domains for analysis. The sizes of HCP-3 domains on *air-2(or207ts)* fibers were more variable than those in wild type. Accordingly, the average size of HCP-3 domains was larger on *air-2(or207ts)* fibers than on wild-type fibers (Figure 6D). Taken together, loss of AIR-2 results in the mis-localization of HCP-3 on chromatin, forming brighter and larger HCP-3 domains.

Discussion

Aurora B/AIR-2 functions have been broadly investigated from yeast to mammalian species (Lampson and Cheeseman, 2011; Hindriksen et al., 2017; Broad and DeLuca, 2020). Due to the pleiotropic roles of Aurora B/AIR-2 in both mitosis and meiosis, the detailed mechanism of how Aurora B/AIR-2 contributes to centromere organization in mitosis is less understood. To avoid meiotic effects, the temperature-sensitive mutant *air-2(or207ts)* was utilized, which enables us to acutely inactivate the function of AIR-2 at any developmental stage, for example after meiosis and just before the first mitosis, by shifting the temperature during worm cultivation (Chakshusmathi et al., 2004). Compared to other strategies for investigating gene and protein function, e.g. RNAi depletion, small-molecule inhibitors, clustered regularly interspaced short palindromic repeats (CRISPR) interference, and auxin-inducible degron system, the temperature-sensitive mutant approach represents a versatile tool that possesses high reversibility, fast thermal response, and applicability to any developmental stage of the model organism.

In the absence of AIR-2 function, multiple phenotypic defects, including disorganized metaphase plate formation, two chromatid masses separation, and chromatin bridges, were
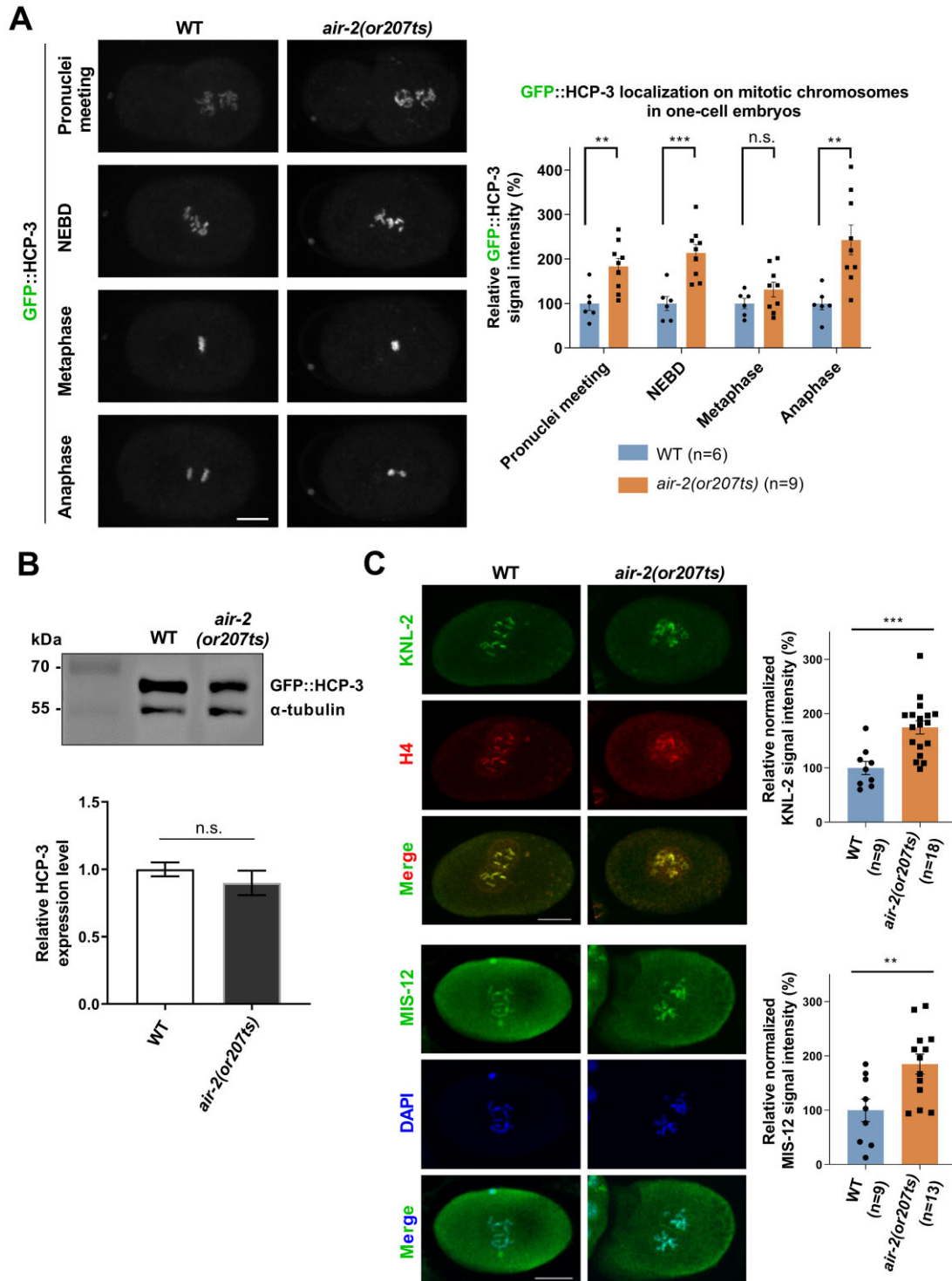
Figure 5 Loss of Aurora B/AIR-2 escalates CENP-A/HCP-3 localization on chromatin. (**A**) Time-lapse images of HCP-3 localization at different mitotic stages. Scale bar, 10 μm. Relative HCP-3 signal intensity in wild-type and *air-2(or207ts)* cells. n: number of one-cell embryos examined. Error bars: 95% CI of the SEM. n.s., not significant; **$P < 0.01$, ***$P < 0.001$, unpaired *t*-test. (**B**) Western blot analysis of GFP::HCP-3 protein expression levels, with α-tubulin as a loading control. The bar chart shows the relative HCP-3 protein level. Three biological replicates were performed. Error bars indicate standard deviation. n.s., not significant, unpaired *t*-test. (**C**) Immunofluorescence staining of KNL-2 and MIS-12 in prometaphase. Scale bar, 10 μm. Normalized KNL-2 (to H4) and MIS-12 (to DAPI) signal intensities in wild-type and *air-2(or207ts)* cells. n: number of one-cell embryos examined. Error bars: 95% CI of the SEM. **$P < 0.01$, ***$P < 0.001$, unpaired *t*-test.
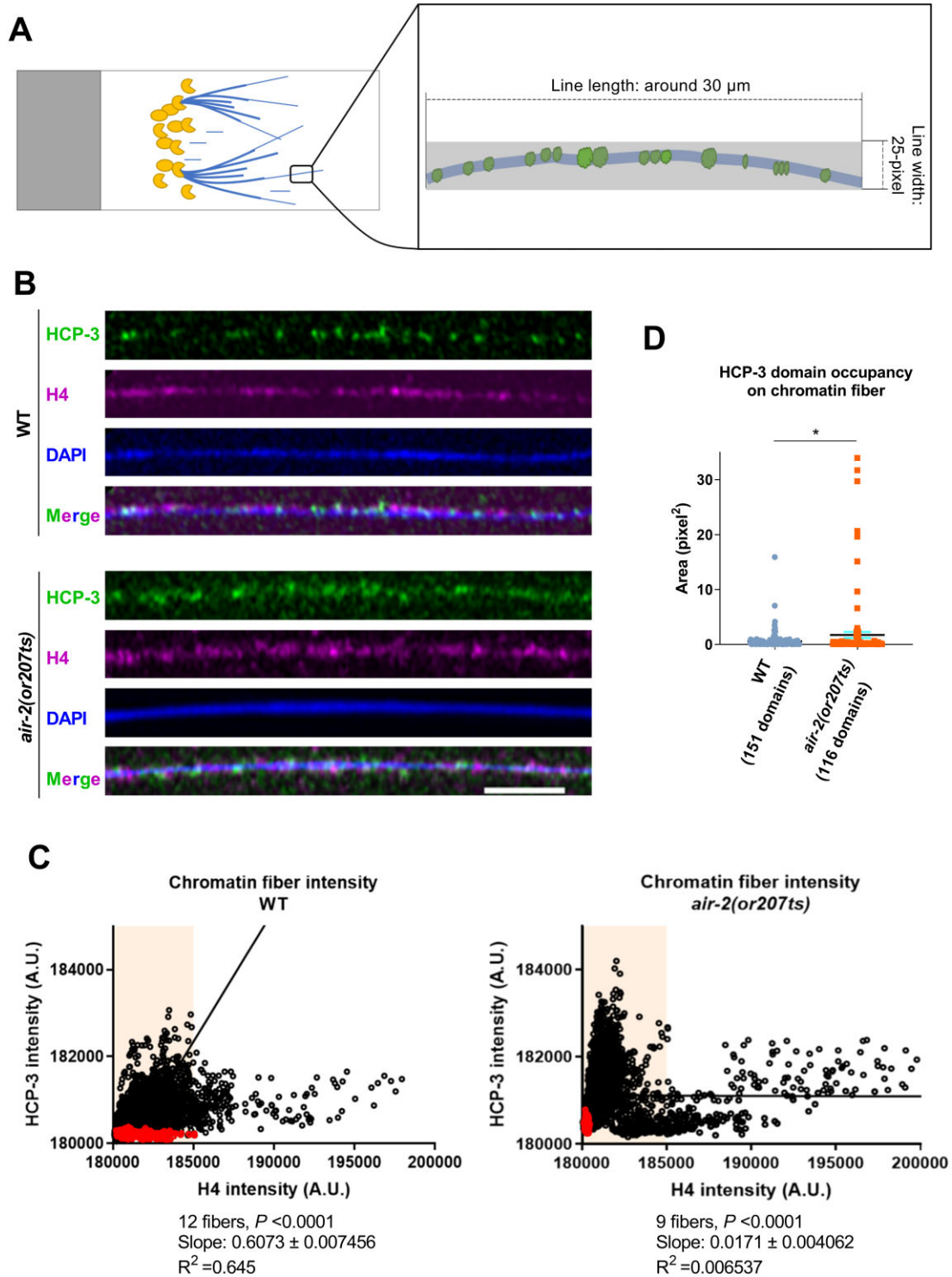
Figure 6 Comparison of centromere localization patterns between wild-type and *air-2(or207ts)* fibers. (**A**) The diagram depicts the method for stretched fiber acquirement and measurement. (**B**) Chromatin fiber images from wild-type and *air-2(or207ts)* embryos. HCP-3 and H4 localization on the DAPI-stained DNA filaments are shown. Scale bar, 5 μm. (**C**) Scatter plots of HCP-3 and H4 average intensities on chromatin fibers. Red dots in each scatter plot indicate the background signal intensities, measured at areas outside the respective fibers. The interval (light orange space) includes the fibers with similar thickness. (**D**) Quantification of HCP-3 domain occupancy on chromatin fibers. Error bars (indicated in cyan color): 95% CI of the SEM. *$P < 0.05$, unpaired *t*-test.

characterized in mitosis (Figure 1B and C). The mitotic division duration (from NEBD to anaphase) was extended in AIR-2-deficient cells (Figure 1D). These findings indicate that AIR-2 is critical for chromosome segregation in mitosis. One plausible explanation for the prolonged process is that the absence of AIR-2 causes a delay in sister centromere resolution (Figure 2B). There is a higher frequency of merotely in prometaphase in *air-2(or207ts)* embryos (Figure 1E and F). As AIR-2 has been verified to function in aberrant attachment correction by a tension-sensing mechanism (Hauf et al., 2003; Funabiki, 2019; McVey et al., 2021), it is reasonable that *air-2(or207ts)* embryos may take longer to repair the erroneous attachments before anaphase ensues. Several processes might account for the increased merotelic attachments in *air-2(or207ts)* embryos, such as the defective sister centromere resolution, defective centromere organization leading to potentially ectopic kinetochores, and the collapsed correction machinery for erroneous spindle–microtubule attachments.

An earlier study in *C. elegans* has elucidated that AIR-2 recruits common subunits of condensin I and condensing II (SMC-2/MIX-1 and SMC-4) to holocentric chromosomes (Hagstrom et al., 2002). Notably, both condensin I and condensin II complexes are critical for chromosome condensation, and lack of condensin affects the rigidity of chromosomes, leading to twisted chromosomes. A previous study suggested that the rise of merotely rate was due to the twisted chromatids caused by decondensed chromosomes (Stear and Roth, 2002). To validate this hypothesis, the mitotic chromosome condensation was quantitively measured in *air-2(or207ts)* embryos. Indeed, condensation in *air-2(or207ts)* cells occurred earlier. Besides, the chromatin looked more compacted in *air-2(or207ts)* cells at the initial condensation stage. However, the final condensation level reached a similar extent in both wild-type and *air-2(or207ts)* cells upon NEBD (Supplementary Figure S1C), which is consistent with condensation measurement reported in Maddox's study (Maddox et al., 2006). Our findings indicate that the condensation level is not severely affected in the absence of AIR-2 activity. The mild condensation dynamic defect resulting from AIR-2 inactivation during prophase is not considered to be the primary reason to cause more merotelic attachments. This is because the initiation of kinetochore–microtubule attachments occurs normally after NEBD.

In concert with Collette et al. (2011), the absence of AIR-2 function resulted in defects in the loading of condensin I to chromosomes in *C. elegans*. Almost 100% of condensin I was diminished on mitotic chromatin when the AIR-2 function was abolished, suggesting that AIR-2 is crucial for targeting condensin I to chromosomes in mitosis (Supplementary Figure S2). Theoretically, the condensin I complex does not cause an effect on sister centromere resolution, since it loads onto chromatids after NEBD when the resolution should be completed already (Hirota et al., 2004; Takao Ono et al., 2004). Thus, we focus on whether and how AIR-2 targets condensin II components to mitotic chromosomes. Different from previous studies (Maddox et al., 2006; Collette et al., 2011), we found that condensin II

component localization to chromosomes was partially affected by AIR-2 in our system (Figure 3). Condensin II component HCP-6 has been determined to play a crucial role in sister centromere resolution, whilst centromeric protein HCP-3 is an upstream factor known to recruit HCP-6 to chromatids (Chan et al., 2004). This may explain why the loss of AIR-2 merely triggered a portion of decrease in HCP-6 level, as AIR-2 and HCP-3 coordinately regulated HCP-6 localization to chromosomes (Figure 4D). Strikingly, cells inactivated of AIR-2 also exhibited a notable decline in the levels of KLE-2 and CAPG-2 to chromatin at specific stages of mitosis. Together with the evidence that condensin components can interact with chromatin independently (Chan et al., 2004), we suspect that AIR-2 has a slightly different time-dependent influence on the loading of all three condensin II subunits (HCP-6, KLE-2, and CAPG-2) in mitosis. Condensin II subunits may have different loading dependencies. A decrease in any of the subunits can impact the overall function of the condensin complex.

Sister centromere resolution is a prerequisite for centromere bipolar orientation organization in prometaphase and later equal chromosome segregation in anaphase. In this study, sister centromere resolution was first discovered to occur upon the paternal and maternal pronuclei meeting in one-cell stage, and the whole process to achieve poleward-facing holocentromere localization was completed before NEBD, prior to microtubule attachment (Figure 2A and B). Furthermore, the initiation of sister centromere resolution was shown to be retarded in *air-2(or207ts)* embryos, with ∼100 sec extension when compared to that in wild-type embryos (Figure 2B). To explore deeper into the mechanism of AIR-2 in sister centromere resolution, we quantitatively categorized the types of centromeres based on the different HCP-3 distribution patterns (Figure 4B and C). Usually, centromeres are displayed as the mono-oriented centromere mode in early prophase and become bipolar-oriented centromere configuration in prometaphase. Almost half of centromeres in *air-2(or207ts)* cells displayed disorganized configuration in prometaphase (Figure 4D). Cells depleted of HCP-6 triggered a higher frequency of disorganized centromere observation in prometaphase when compared to that in the single *air-2* mutant. The resolution frequency of *air-2(or207ts)hcp-6(RNAi)* was similar to that of *hcp-6(RNAi)*, suggesting that AIR-2 mainly acts through HCP-6 (Figure 4D). On the other hand, HCP-6 is regulated by AIR-2 and HCP-3 coordinately. Given that there was still a portion of bipolar-oriented centromeres scored in *air-2(or207ts)hcp-6(RNAi)* embryos, a reasonable speculation is that cells may have a compensation pathway to assist sister centromere resolution when both AIR-2 or HCP-3 pathways are blocked. Previous work suggests that the spindle microtubules attaching to kinetochores could partly rescue the unresolved centromeres (Moore et al., 2005). We used nocodazole for microtubule depolymerization, to examine the role of microtubule attachments in assisting centromere resolution. We depleted both AIR-2 and HCP-6, and inhibited microtubule function, and found that nearly 100% of centromeres displayed the disorganized configuration
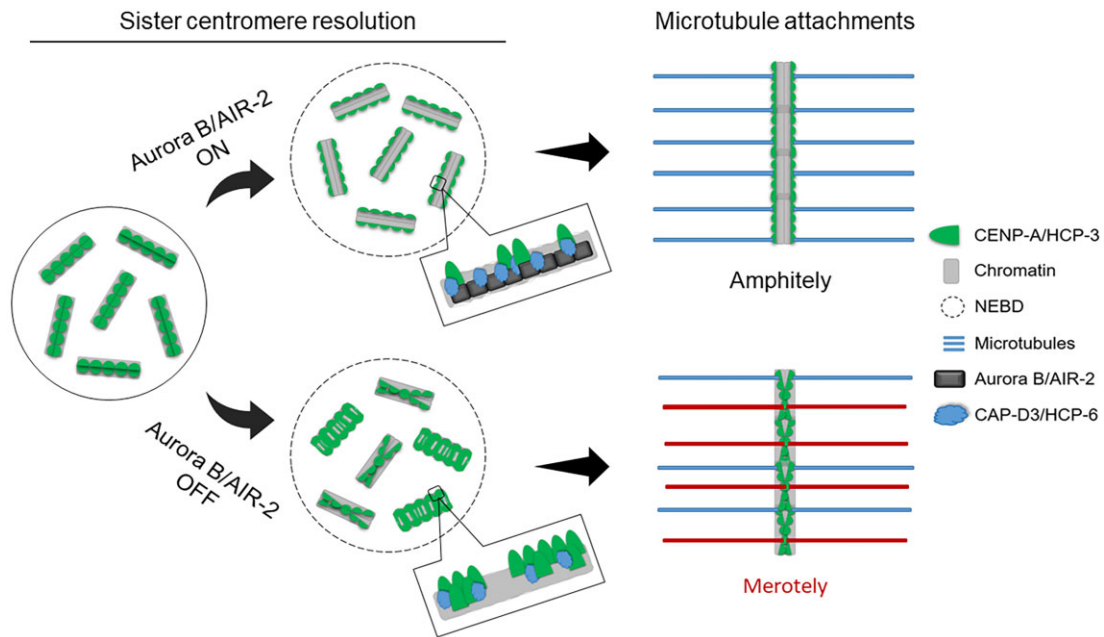
Figure 7 Schematic depiction of Aurora B/AIR-2 functions in centromere organization. Normally, AIR-2 and HCP-3 coordinately recruit HCP-6 to centromeric chromatin, safeguarding the correct resolution of sister centromeres before NEBD. Then, the spindle microtubules attach bipolar-oriented sister centromeres to achieve amphitelic attachments (indicated by the MTs in blue color). When AIR-2 is inactivated, a portion of HCP-6 is lost on the centromeric chromatin, leading to the aberrant sister centromere resolution and mis-localization of centromere protein. These defects may trigger merotelic attachments between MTs and centromeres (indicated by the MTs in red color), giving rise to mis-segregation of sister chromatids in anaphase and even aneuploidy occurring in daughter cells.

(Figure 4D). Consistent with the previous finding (Moore et al., 2005), the result verified that the spindle microtubules can partly rescue the unresolved centromere in prometaphase. Based on the search-and-capture mechanism of dynamic microtubules, we suggest that microtubules can attach with those partially resolved centromeres in late prometaphase. By pulling the sister chromatids with tension, it helps to orient the unresolved parts of sister centromeres. Thereby, we conclude that condensin II is the main regulator for correct sister centromere resolution, while spindle microtubules may serve as the savior to assist centromere resolution if the HCP-6-recruiting pathways are disrupted in the early stage of mitosis.

Intriguingly, AIR-2 was found to regulate HCP-3 localization to chromatin, but not on the protein expression level, as western blotting result showed the total protein levels were similar in wild-type and *air-2(or207ts)* cells (Figure 5A and B). To further investigate the potential reason for the HCP-3 abnormal localization on chromatin, we examined the HCP-3 domain occupancy on chromatin fibers. Fibers extracted from *air-2(or207ts)* embryos exhibited more prominent HCP-3 foci, which were assembled in a denser pattern (Figure 6B). One possible explanation for these phenotypes is that HCP-3 mis-localizes on chromatin, forming larger clusters of HCP-3 domains. The visualization of HCP-3 domain expansion on *air-2(or207ts)* chromatin fibers convinces us that loss of AIR-2 alters the localization pattern of centromere on chromatin. The mis-localized HCP-3 potentially attracts additional kinetochore proteins to chromatin, leading to the formation of ectopic kinetochore complexes. Our quantification analysis verified an increase of centromeric proteins (CENP-A/HCP-3 and M18BP1/KNL-2) and kinetochore protein (MIS-12) on chromosomes in the absence of AIR-2 activity (Figure 5C). The localization of MIS-12 is demonstrated to depend on CENP-C/HCP-4 (Oegema and Hyman, 2006; Cheeseman et al., 2008). Surprisingly, our findings indicate that AIR-2 does not directly influence HCP-4 but instead affects MIS-12 (Figure 5C; Supplementary Figure S3B), suggesting that some MIS-12 may bypass CENP-C requirement in an unknown mechanism. Additionally, it raises the question of whether centromere mis-localization, coupled with increased kinetochore localization, is more likely to trigger erroneous attachments in cells, thus leading to the delay in mitotic progression and chromosome mis-segregation. Indeed, evidence of ectopic kinetochore assembly to form merotelic attachments was broadly discussed in previous studies (Heun et al., 2006; Gascoigne et al., 2011; Tovini et al., 2023). Together with frequently merotelic attachments observed in AIR-2-deficient embryos, it is suggested that one of AIR-2's functions is to regulate the localization of centromeres on chromatin, ensuring the accurate assembly of kinetochores to prevent merotelic attachments with microtubules in early mitosis (Figure 7).

Loss of Aurora B/AIR-2 function triggers a significant adverse impact on several mitotic events, such as centromere organization, centromere bipolar orientation, and chromosome

segregation. The understanding of the relationship between centromere deposition and sister centromere resolution is still limited. The mechanism of how Aurora B/AIR-2 regulates these processes is also unclear. However, our phosphoproteomic analysis of nematodes in response to Aurora B/AIR-2 kinase inactivation identified that HCP-6 belongs to the down-regulated phosphopeptide group (unpublished data). Nevertheless, further analysis of Aurora B/AIR-2-dependent phosphorylation will help us understand whether different condensin components and centromeric proteins are target substrate proteins. In sum, the process of centromere organization regulated by Aurora B/AIR-2 is summarized in Figure 7. Our study unravels an additional role of Aurora B/AIR-2 in preventing merotelic attachments through regulating correct sister centromere resolution and proper centromere localization in the early stage of mitosis, which further guarantee that chromosomes achieve bipolar orientation before segregation.

Materials and methods

Worm strains and maintenance

For Petri dish culture, worms were grown and maintained at 22°C on freshly made MYOB plates (0.55 g Tris-Cl, 0.24 g Tris-OH, 3.1 g Bacto Peptone, 8 mg cholesterol, and 2.0 g NaCl; mixed with 1 L Milli-Q water) seeded with OP50 *Escherichia coli* bacteria. Notably, the temperature-sensitive worms were kept at 15°C for maintenance. Worm strains used in this study are listed in Supplementary Table S1.

Double-stranded RNA (dsRNA) synthesis and RNAi

Approximately 1000 base pairs of the coding region of targeted genes were amplified from N2 *C. elegans* cDNA using forward and reverse primers with $5'$ flanking T3 promoter sequence (AATTAACCCTCACTAAAGGG) and T7 promoter sequence (TAATACGACTCACTATAGGG), respectively. Primers resulted in only one specific product band with the expected size were used (Supplementary Table S2). Purified polymerase chain reaction products were subjected to *in vitro* transcription using the MEGAscript T3/T7 Transcription Kit (Life Technologies). Reaction products were digested with TURBO DNase at 37°C for 15 min and purified using the MEGAclear Kit (Life Technologies). Eluates were mixed with an equal volume of TE buffer (0.5 M ethylenediaminetetraacetic acid (EDTA) and 1 M Tris-Cl), followed by incubation at 68°C for 10 min and 37°C for 30 min to generate dsRNA. The yield of dsRNA was assessed and finally concentrated to 1 mg/ml. RNAi knockdown was achieved by injecting 1 mg/ml dsRNA into L4 hermaphrodites. They were then transferred to fresh EZ worm plates with OP50 for 24 h at 15°C or 22°C.

Immunofluorescence staining

Embryos harvested from bleaching gravid worms were seeded on the poly-L-lysine-coated slides with cover glass. After being freeze-cracked in liquid nitrogen, slides were immediately fixed in chilled methanol at −20°C for 30 min, rehydrated in phosphate buffered saline (PBS) buffer (137 mM NaCl, 2.7 mM KCL, 10 mM Na_2HPO_4, and 1.8 mM KH_2PO_4) for 10 min, and further incubated in blocking solution (4% bovine serum albumin and 0.1% Triton X-100 in PBS) at room temperature for 10 min. Incubation of the primary antibody against HCP-3 (1:500; Novus 29540002 SDQ0804), GFP (1:500; Novus #NB600308), α-tubulin (1:1000; Abcam #ab7291), H4 (1:500; Abcam #ab31830), KNL-2 (1:500; a gift from the Desai Lab), or MIS-12 (1:1000; SDI #35550002) was performed at 4°C overnight. Slides were washed with PBS buffer containing 0.1% Triton X-100 (PBS-T), followed by FITC- or Cy3-conjugated secondary antibody (1:200; Jackson ImmunoResearch Laboratories) incubation at 37°C for 1 h. Again, slides were washed with PBS-T before $4'$,6-diamidino-2-phenylindole (DAPI) incubation and mounting (Prolong Diamond Antifade Mountant, Thermo Fisher Scientific). Embryos were captured using Zeiss LSM880 inverted confocal microscope system (63× 1.4 numerical aperture (NA) oil objective, 32-channel GaAsp PMTs Airyscan detector) in Z-stack images at 0.2 μm interval.

Western blotting

Embryos were lysed in 200 μl M9/0.1% Triton X-100 containing the EDTA-free protease inhibitor tablet (Roche) using water bath sonication at 4°C for 30 min. After boiling in 4× sample buffer (8% sodium dodecyl sulphate (SDS), 0.04% bromophenol blue, 240 mM Tris-Cl, 40% glycerol, and 5% β-mercaptoethanol) at 100°C for 10 min, ~30 μg proteins were loaded in each lane for SDS–polyacrylamide gel electrophoresis and transferred to polyvinylidene difluoride membrane (Millipore) by the wet electroblotting system. The membranes were blocked with 5% non-fat milk in TBS-T buffer (20 mM Tris-Cl, 150 mM NaCl, and 0.1% Tween-20) for 1 h and then probed by using antibodies against α-tubulin (1:1000; Abcam ab7291 DM1A), HCP-3 (1:1000; Novus SDQ0804 or 29540002) at 4°C overnight with agitation. After washing with TBS-T buffer, immunoblots were subjected to HRP-conjugated antibody incubation (1:2000; Bio-Rad ab1706515 or ab1706516) at room temperature for 1 h, then washed again. Protein signals were developed by Amersham ECL Prime Western blotting detection reagent (GE Healthcare Life Sciences) and detected by Alliance Q9 Advanced Chemiluminescence Imager. The band signal intensities were quantified using ImageJ software. The protein band was selected and quantified by fitting a rectangle around the band. To calculate the fold change of the protein level, the band intensity of the protein was first normalized to the loading control (α-tubulin) and then compared to normalized signal intensity in the wild-type group.

Shifting time determination and live-cell imaging

To prevent meiotic defects that can inherit into mitosis due to AIR-2 inactivation, it is necessary to shift the culture temperature to 25°C only after the sister chromatids have segregated in meiotic anaphase II. The time between meiotic anaphase II (from the end of metaphase II stage) and the meeting of paternal and maternal pronuclei is typically 10 min (McCarter et al., 1999; Sonneville and Gonczy, 2004; Oegema and Hyman, 2006). Hence, the temperature upshift must be

applied within 10 min prior to acquiring images of pronuclei meeting in the first cell division.

The preparation and mounting of worm embryos were carried out as described (Powers, 2010). Images were acquired using Perkin Elmer Ultraview Vox spinning disk confocal microscope system (60× 1.4 NA oil lens) or Zeiss LSM880 system (40× 1.4 NA oil objective, 32-channel GaAsp PMTs Airyscan detector). For imaging of the temperature-sensitive strain, a stage-top incubator (Tokai Hit) was assembled to maintain an optimal imaging environment with precise temperature control. The imaging parameters were kept consistent within the same experiment. For the spinning disk confocal microscope system, 200-ms and 400-ms exposures at the 488-nm and 543-nm channels were used as acquisition conditions, respectively. Time-lapse images were captured in stacks of 11 sections along the Z-axis at 1.5 µm interval. For the LSM880 system, 488-nm and 561-nm channels were used as acquisition conditions. Time-lapse images were captured in stacks of nine sections along the Z-axis at 1.5 µm interval.

Chromatin fiber assay

Embryos were treated with yatalase (7.5 mg/ml) for 10 min with rotation, followed by a single wash in embryo buffer (25 mM HEPES, 118 mM NaCl, 48 mM KCl, 2 mM $CaCl_2·2H_2O$, and 2 mM $MgCl_2·6H_2O$). Then, 5 µl of embryo suspension was spread by streaking a line on the glass slide and allowed to reach a semi-dry state. The embryo lysis and chromatin fiber stretching were performed based on the previous protocol (Dunleavy et al., 2011). Slides were incubated in lysis buffer (10 mM Tris, 1% Triton-X-100, 200 mM NaCl, and 500 mM urea) for 20 min at room temperature. Slides were then pulled out vertically slowly. After washing with PBS once, the slides were placed back in the lysis buffer to lyse for another 20 min. Afterwards, slides were immediately fixed in cold methanol for 30 min at −20°C and further proceeded with immunofluorescence staining. All fiber images were acquired using Zeiss LSM880 inverted confocal microscope system (40× 1.4 NA oil objective, 32-channel GaAsp PMTs Airyscan detector) in stacks of 18 sections along the Z-axis at 0.3 µm interval.

Fiber images were analyzed by ImageJ software. A segmented line (25 pixel wide, 30 µm long) was drawn on the fiber and the average HCP-3 and H4 intensities among the line were exported and further plotted with a scatter diagram. Similar thickness fibers were selected and straightened to be the lined structure. Then, a threshold (GFP::HCP-3 intensity >181000 A.U.) was set to exclude those HCP-3 background pixels. Regions of interest of HCP-3 pixels determined by ImageJ using Analyze Particles function (size: 5–200; circularity: 0.01–1.00) were characterized as HCP-3 domain occupancy on chromatin fibers.

Image quantification analysis

All images were quantified using ImageJ software. For live-cell imaging, Z-stack images were subjected to maximum intensity projection before analysis. For immunofluorescence staining, Z-stack images were proceeded with sum intensity projection before analysis, except for the α-tubulin staining images, in which a single section was used for merotelic attachment quantification. To be specific, a fixed area fitting and enclosing all chromosomes was selected as A, and a larger area embracing area A within the cytoplasm was defined as B. For each channel, integrated signal intensities in A and B were measured as A1 and B1, separately. The average background intensity (C) was calculated as $\frac{(B1-A1)}{(B-A)}$. The average signal intensity on chromosomes within area A was measured as $\frac{(A1-C*A)}{A}$.

Supplementary material

Supplementary material is available at *Journal of Molecular Cell Biology* online.

Conflict of interest: none declared.

Author contributions: Y.W. and K.W.Y.Y. contributed to conceptualization and visualization and wrote the original draft; Y.W. was involved in investigation and formal analysis; Y.W., C.Y.Y.W., and K.W.Y.Y. contributed to methodology, writing, review, and editing; and K.W.Y.Y. acquired funding and contributed to resources, supervision, and project administration. All authors read and approved the final manuscript.

References

Adams, R.R., Maiato, H., Earnshaw, W.C., et al. (2001). Essential roles of Drosophila inner centromere protein (Incenp) and Aurora B in histone H3 phosphorylation, metaphase chromosome alignment, kinetochore disjunction, and chromosome segregation. J. Cell Biol. *153*, 865–880.

Andrews, P.D., Ovechkina, Y., Morrice, N., et al. (2004). Aurora B regulates MCAK at the mitotic centromere. Dev. Cell *6*, 253–268.

Baldini, E., Tuccilli, C., Sorrenti, S., et al. (2016). Aurora kinases: new molecular targets for the therapy of aggressive thyroid cancers. In: Bankovic, J. (ed.). Anti-Cancer Drugs—Nature, Synthesis and Cell. IntechOpen, http://dx.doi.org/10.5772/64597

Brenner, S., Pepper, D., Berns, M.W., et al. (1981). Kinetochore structure, duplication, and distribution in mammalian cells: analysis by human autoantibodies from scleroderma patients. J. Cell Biol. *91*, 95–102.

Broad, A.J., and DeLuca, J.G. (2020). The right place at the right time: Aurora B kinase localization to centromeres and kinetochores. Essays Biochem. *64*, 299–311.

Buchwitz, B.J., Ahmad, K., Moore, L.L., et al. (1999). A histone-H3-like protein in C. elegans. Nature *401*, 547–548.

Carmena, M., Wheelock, M., Funabiki, H., et al. (2012). The chromosomal passenger complex (CPC): from easy rider to the godfather of mitosis. Nat. Rev. Mol. Cell Biol. *13*, 789–803.

C. elegans Sequencing Consortium (1998). Genome sequence of the nematode C. elegans: a platform for investigating biology. Science *282*, 2012–2018.

Chakshusmathi, G., Mondal, K., Lakshmi, G.S., et al. (2004). Design of temperature-sensitive mutants solely from amino acid sequence. Proc. Natl Acad. Sci. USA *101*, 7925–7930.

Chan, R.C., Severson, A.F., and Meyer, B.J. (2004). Condensin restructures chromosomes in preparation for meiotic divisions. J. Cell Biol. *167*, 613–625.

Cheeseman, I.M., Chappie, J.S., Wilson-Kubalek, E.M., et al. (2006). The conserved KMN network constitutes the core microtubule-binding site of the kinetochore. Cell *127*, 983–997.

Cheeseman, I.M., Hori, T., Fukagawa, T., et al. (2008). KNL1 and the CENP-H/I/K complex coordinately direct kinetochore assembly in vertebrates. Mol. Biol. Cell *19*, 587–594.

Cimini, D. (2008). Merotelic kinetochore orientation, aneuploidy, and cancer. Biochim. Biophys. Acta *1786*, 32–40.

Collette, K.S., Petty, E.L., Golenberg, N., et al. (2011). Different roles for Aurora B in condensin targeting during mitosis and meiosis. J. Cell Sci. *124*, 3684–3694.

Csankovszki, G., Collette, K., Spahl, K., et al. (2009). Three distinct condensin complexes control C. elegans chromosome dynamics. Curr. Biol. *19*, 9–19.

De Rop, V., Padeganeh, A., and Maddox, P.S. (2012). CENP-A: the key player behind centromere identity, propagation, and kinetochore assembly. Chromosoma *121*, 527–538.

Doodhi, H., Kasciukovic, T., Clayton, L., et al. (2021). Aurora B switches relative strength of kinetochore–microtubule attachment modes for error correction. J. Cell Biol. *220*, e202011117.

Doodhi, H., and Tanaka, T.U. (2022). Swap and stop—kinetochores play error correction with microtubules. Bioessays *44*, e2100246.

Dunleavy, E.M., Almouzni, G., and Karpen, G.H. (2011). H3.3 is deposited at centromeres in S phase as a placeholder for newly assembled CENP-A in G_1 phase. Nucleus *2*, 146–157.

Fire, A., Xu, S., Montgomery, M.K., et al. (1998). Potent and specific genetic interference by double-stranded RNA in Caenorhabditis elegans. Nature *391*, 806–811.

Funabiki, H. (2019). Correcting aberrant kinetochore microtubule attachments: a hidden regulation of Aurora B on microtubules. Curr. Opin. Cell Biol. *58*, 34–41.

Gascoigne, K.E., Takeuchi, K., Suzuki, A., et al. (2011). Induced ectopic kinetochore assembly bypasses the requirement for CENP-A nucleosomes. Cell *145*, 410–422.

Gassmann, R., Rechtsteiner, A., Yuen, K.W., et al. (2012). An inverse relationship to germline transcription defines centromeric chromatin in C. elegans. Nature *484*, 534–537.

Giet, R., and Glover, D.M. (2001). Drosophila Aurora B kinase is required for histone H3 phosphorylation and condensin recruitment during chromosome condensation and to organize the central spindle during cytokinesis. J. Cell Biol. *152*, 669–682.

Hagstrom, K.A., Holmes, V.F., Cozzarelli, N.R., et al. (2002). C. elegans condensin promotes mitotic chromosome architecture, centromere organization, and sister chromatid segregation during mitosis and meiosis. Genes Dev. *16*, 729–742.

Hauf, S., Cole, R.W., LaTerra, S., et al. (2003). The small molecule Hesperadin reveals a role for Aurora B in correcting kinetochore–microtubule attachment and in maintaining the spindle assembly checkpoint. J. Cell Biol. *161*, 281–294.

He, D., and Brinkley, B.R. (1996). Structure and dynamic organization of centromeres/prekinetochores in the nucleus of mammalian cells. J. Cell Sci. *109*, 2693–2704.

Heun, P., Erhardt, S., Blower, M.D., et al. (2006). Mislocalization of the Drosophila centromere-specific histone CID promotes formation of functional ectopic kinetochores. Dev. Cell *10*, 303–315.

Hindriksen, S., Lens, S.M.A., and Hadders, M.A. (2017). The ins and outs of Aurora B inner centromere localization. Front. Cell Dev. Biol. *5*, 112.

Hirano, T. (2016). Condensin-based chromosome organization from bacteria to vertebrates. Cell *164*, 847–857.

Hirota, T., Gerlich, D., Koch, B., et al. (2004). Distinct functions of condensin I and II in mitotic chromosome assembly. J. Cell Sci. *117*, 6435–6445.

Jenni, S., and Harrison, S.C. (2018). Structure of the DASH/Dam1 complex shows its role at the yeast kinetochore–microtubule interface. Science *360*, 552–558.

Kaitna, S., Pasierbek, P., Jantsch, M., et al. (2002). The Aurora B kinase AIR-2 regulates kinetochores during mitosis and is required for separation of homologous chromosomes during meiosis. Curr. Biol. *12*, 798–812.

Kalantzaki, M., Kitamura, E., Zhang, T., et al. (2015). Kinetochore–microtubule error correction is driven by differentially regulated interaction modes. Nat. Cell Biol. *17*, 421–433.

Kim, Y., Park, Y., Hwang, J., et al. (2018). Comparative genomic analysis of the human and nematode Caenorhabditis elegans uncovers potential reproductive genes and disease associations in humans. Physiol. Genomics *50*, 1002–1014.

Krenn, V., and Musacchio, A. (2015). The Aurora B kinase in chromosome bi-orientation and spindle checkpoint signaling. Front. Oncol. *5*, 225.

Kuhn, J., and Dumont, S. (2017). Spindle assembly checkpoint satisfaction occurs via end-on but not lateral attachments under tension. J. Cell Biol. *216*, 1533–1542.

Kunitoku, N., Sasayama, T., Marumoto, T., et al. (2003). CENP-A phosphorylation by Aurora-A in prophase is required for enrichment of Aurora-B at inner centromeres and for kinetochore function. Dev. Cell *5*, 853–864.

Lampson, M.A., and Cheeseman, I.M. (2011). Sensing centromere tension: Aurora B and the regulation of kinetochore function. Trends Cell Biol. *21*, 133–140.

Lipp, J.J., Hirota, T., Poser, I., et al. (2007). Aurora B controls the association of condensin I but not condensin II with mitotic chromosomes. J. Cell Sci. *120*, 1245–1255.

Maddox, P.S., Portier, N., Desai, A., et al. (2006). Molecular analysis of mitotic chromosome condensation using a quantitative time-resolved fluorescence microscopy assay. Proc. Natl Acad. Sci. USA *103*, 15097–15102.

McCarter, J., Bartlett, B., Dang, T., et al. (1999). On the control of oocyte meiotic maturation and ovulation in Caenorhabditis elegans. Dev. Biol. *205*, 111–128.

McHugh, T., Zou, J., Volkov, V.A., et al. (2019). The depolymerase activity of MCAK shows a graded response to Aurora B kinase phosphorylation through allosteric regulation. J. Cell Sci. *132*, jcs228353.

McVey, S.L., Cosby, J.K., and Nannas, N.J. (2021). Aurora B tension sensing mechanisms in the kinetochore ensure accurate chromosome segregation. Int. J. Mol. Sci. *22*, 8818.

Moore, L.L., and Roth, M.B. (2001). HCP-4, a CENP-C-like protein in Caenorhabditis elegans, is required for resolution of sister centromeres. J. Cell Biol. *153*, 1199–1208.

Moore, L.L., Stanvitch, G., Roth, M.B., et al. (2005). HCP-4/CENP-C promotes the prophase timing of centromere resolution by enabling the centromere association of HCP-6 in Caenorhabditis elegans. Mol. Cell. Biol. *25*, 2583–2592.

Oegema, K., and Hyman, A.A. (2006). Cell division. In: WormBook: The Online Review of C. elegans Biology. Pasadena, CA: WormBook, https://doi.org/10.1895/wormbook.1.72.1

Ohi, R., Sapra, T., Howard, J., et al. (2004). Differentiation of cytoplasmic and meiotic spindle assembly MCAK functions by Aurora B-dependent phosphorylation. Mol. Biol. Cell *15*, 2895–2906.

Powers, J.A. (2010). Live-cell imaging of mitosis in Caenorhabditis elegans embryos. Methods *51*, 197–205.

Schumacher, J.M., Golden, A., and Donovan, P.J. (1998). AIR-2: an Aurora/Ipl1-related protein kinase associated with chromosomes and midbody microtubules is required for polar body extrusion and cytokinesis in Caenorhabditis elegans embryos. J. Cell Biol. *143*, 1635–1646.

Severson, A.F., Hamill, D.R., Carter, J.C., et al. (2000). The aurora-related kinase AIR-2 recruits ZEN-4/CeMKLP1 to the mitotic spindle at metaphase and is required for cytokinesis. Curr. Biol. *10*, 1162–1171.

Sonneville, R., and Gonczy, P. (2004). zyg-11 and cul-2 regulate progression through meiosis II and polarity establishment in C. elegans. Development *131*, 3527–3543.

Stear, J.H., and Roth, M.B. (2002). Characterization of HCP-6, a C. elegans protein required to prevent chromosome twisting and merotelic attachment. Genes Dev. *16*, 1498–1508.

Takao Ono, Y.F., Spector, D.L., and Hirano, Tatsuya. (2004). Spatial and temporal regulation of condensins I and II in mitotic chromosome assembly in human cells. Mol. Biol. Cell *15*, 3296–3308.

Takemoto, A., Murayama, A., Katano, M., et al. (2007). Analysis of the role of Aurora B on the chromosomal targeting of condensin I. Nucleic Acids Res. *35*, 2403–2412.

Tanaka, T.U. (2010). Kinetochore–microtubule interactions: steps towards bi-orientation. EMBO J. *29*, 4070–4082.

Tovini, L., Johnson, S.C., Guscott, M.A., et al. (2023). Targeted assembly of ectopic kinetochores to induce chromosome-specific segmental aneuploidies. EMBO J. *42*, e111587.

Trivedi, P., and Stukenberg, P.T. (2016). A centromere-signaling network underlies the coordination among mitotic events. Trends Biochem. Sci. *41*, 160–174.

Walczak, C.E., and Heald, R. (2008). Mechanisms of mitotic spindle assembly and function. Int. Rev. Cytol. *265*, 111–158.

Wang, Y., Wu, L., and Yuen, K.W.Y. (2022). The roles of transcription, chromatin organisation and chromosomal processes in holocentromere establishment and maintenance. Semin. Cell Dev. Biol. *127*, 79–89.

Zeitlin, S.G., Shelby, R.D., and Sullivan, K.F. (2001). CENP-A is phosphorylated by Aurora B kinase and plays an unexpected role in completion of cytokinesis. J. Cell Biol. *155*, 1147–1158.